

The Impact of Polydispersity and Molecular Weight on the Order–Disorder Transition in Poly(3-hexylthiophene)

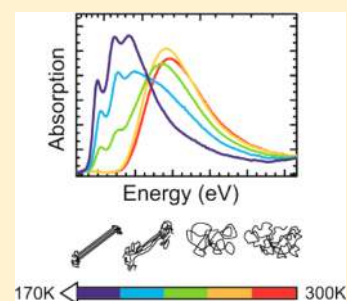
Fabian Panzer,^{†,‡} Heinz Bässler,[‡] Ruth Lohwasser,^{‡,§} Mukundan Thelakkat,^{‡,§} and Anna Köhler^{*,†,‡}

[†]Experimental Physics II, [‡]Bayreuth Institute of Macromolecular Science, and [§]Applied Functional Polymers, Macromolecular Chemistry 1, University of Bayreuth, 95540 Bayreuth, Germany

Supporting Information

ABSTRACT: Conjugated poly(3-hexylthiophene) (P3HT) chains are known to exist at least in two distinct conformations: a coiled phase and a better ordered aggregated phase. Employing steady state absorption and fluorescence spectroscopy, we measure the course of aggregation of P3HT in tetrahydrofuran (THF) solution within a temperature range of 300 K to 170 K. We show that aggregation is a temperature controlled process, driven by a thermodynamic order–disorder transition. The transition temperature increases with the molecular weight of the chains and can be rationalized in the theory of Sanchez. This implies a smearing out of the phase transition in samples with increasing polydispersity and erodes the signature of a first order phase transition. The detection of a hysteresis when undergoing cooling/heating cycles further substantiates this reasoning.

SECTION: Glasses, Colloids, Polymers, and Soft Matter



It is well-known that upon cooling a solution of a conjugated polymer such as polydiacetylene,^{1,2} poly(*p*-phenylenevinylene),^{3,4} polyfluorene⁵ and polythiophene,^{6–8} aggregation occurs. A signature of this phenomenon is the red-shift of absorption and fluorescence spectra accompanied by spectral narrowing. This indicates that in the aggregated phase, the polymer chains are more extended and consequently more ordered. Since in conjugated polymers change in carrier transport is predominantly disorder-controlled, there is a strong endeavor⁹ to understand how to introduce short-range order in electronic devices such as field-effect transistors, organic solar cells, or organic light-emitting diodes (OLEDs) with conjugated polymers as active materials. Since the polymer films are usually processed from solution, strategies are needed toward the formation of ordered structures that exist already in solution and are preserved during solution processing.¹⁰ To this end, we characterize aggregation in solution of poly(3-hexylthiophene) (P3HT), which is a preferred material used for efficient organic solar cells. Stimulated by preceding work on poly(2-methoxy-5-(2'-ethyl-hexoxy)-1,4-phenylene-vinylene) (MEH-PPV) in solution, we studied the aggregation of P3HT in tetrahydrofuran (THF) solution as a function of temperature, molecular weight, and polydispersity. In essence we find that aggregation is, in principle, a first-order transition from a coil to an ordered phase that is smeared out with progressing polydispersity of the chains because the transition temperature depends on molecular weight.

For our studies, we used P3HTs synthesized by a modified Grignard metathesis reaction method as described elsewhere.¹¹ Due to this synthetic method, the samples have a very low polydispersity index (PDI) and thus a very narrow molar mass distribution. The number-average molecular weight (M_n) and the weight-average molecular weight (M_w) were measured by

gel permeations chromatography (GPC) in THF with polystyrene as the calibration standard as well as matrix-assisted laser desorption ionization-time-of-flight mass spectroscopy (MALDI-TOF MS). The polydispersity indices of the low PDI samples were obtained by the GPC data, while the numbers of repeating units, i.e., the degree of polymerization (DP), were determined from the MALDI-TOF measurements, within an experimental uncertainty of 2 repeating units. Commercial P3HT (P3HT-COM) was purchased from American Dye Sources Ltd. (ADS), Canada, and shows a comparable molecular weight to P3HT-19, but a higher PDI of 2.0. Table 1 gives an overview of the relevant properties of the

Table 1. Overview of the Used Materials and Their Corresponding Properties: The Number-Average Molecular Weight (M_n) (Obtained by Both GPC and MALDI-TOF Measurements), Weight-Average Molecular Weight (M_w), Resulting Polydispersity Index ($PDI = M_w/M_n$), and Degree of Polymerisation (DP) (Obtained by MALDI-TOF Measurements)

method	GPC			MALDI-TOF MS		
	notation	M_n (g/mol)	M_w (g/mol)	PDI	M_n (g/mol)	DP
P3HT-5		5100	6300	1.22	3200	19
P3HT-11		11 300	12 500	1.11	7100	43
P3HT-19		18 600	21 600	1.16	12 400	74
P3HT-34		34 200	39 400	1.15	24 000	144
P3HT-COM		18 800	38 400	2.04	n.a.	n.a.

Received: May 19, 2014

Accepted: July 17, 2014

Published: July 17, 2014

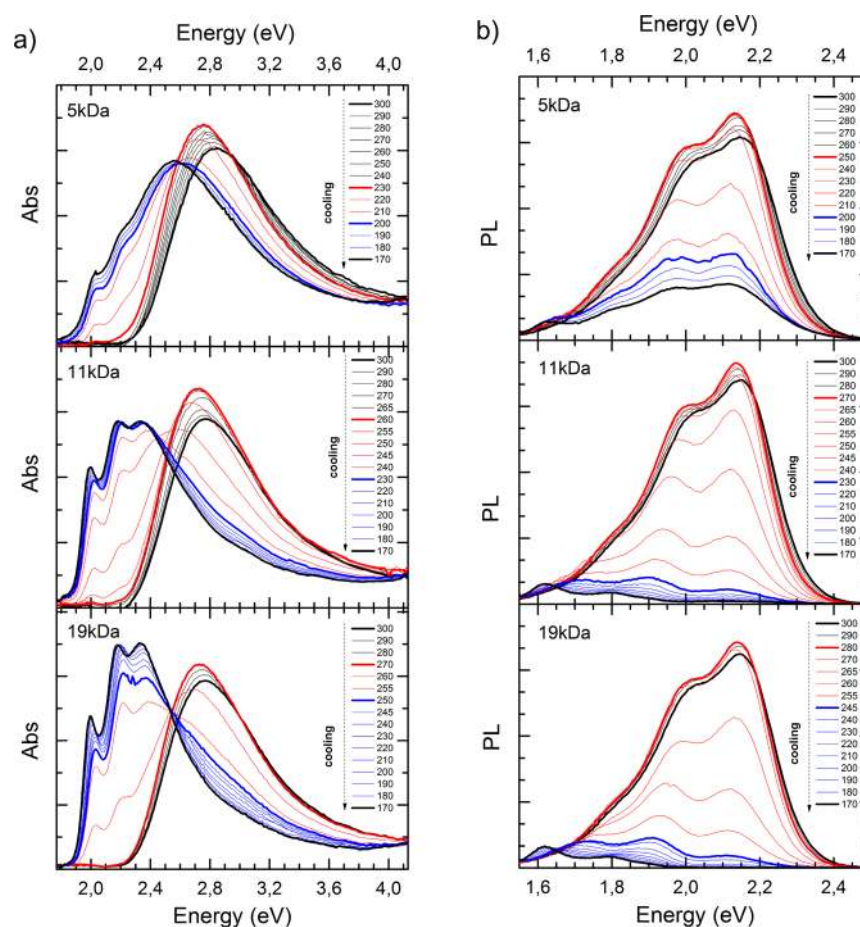


Figure 1. Temperature-dependent absorption (a) as well as corresponding emission spectra (b) for the three Polymers P3HT-5100 (top), P3HT-11 (middle) and P3HT-19 (bottom) in THF, differing in their molecular weight. The spectra are taken from 300 to 170 K in steps of 10 K (usually) or 5 K (near the transition temperature).

used materials including the notation used. We like to note that in the P3HT series used here, the polymer chains do not fold up to a size-exclusion chromatography (SEC) molecular weight of ~ 20 kg/mol (MALDI ~ 12 kg/mol) both in bulk and in thin films on cooling from melt.¹²

All samples were dissolved in THF at a concentration of 0.1 mg/mL. To ensure that all of the polymer chains are completely dissolved, the solutions were heated to 40–50 °C and stirred for about 10 to 30 min, depending on the molecular weight. Absorption and emission spectra at different temperatures were recorded with a home-built setup. The solutions were filled into a fused silica cuvette with 1 mm path length and put into a temperature-controlled continuous flow cryostat (Oxford instruments). In order to minimize the light intensity impinging on the sample, we use two correlated monochromators for incident as well as transmitted light. The latter is recorded by a silicon diode and a lock-in-amplifier.

For emission measurements, the xenon lamp and the first monochromator are replaced via a shutter by a diode laser with an excitation wavelength at 405 nm (3.06 eV), exciting the sample at a shallow angle. Emission is recorded by the same detection unit. This ensures recording absorption and fluorescence spectra at the same sample spot and temperature immediately after one another. All spectra were corrected for the transmission of the setup, using an oriel calibration lamp. Sample heating or cooling was done in a stepwise fashion with a heating or cooling rate of 2K per min and waiting 45 min

before taking the measurement at a given temperature. Absorption as well as emission spectra for the three polymers with different molecular weight and low polydispersity (P3HT-19, P3HT-11, and P3HT-5) were measured within the temperature range from 300 to 170 K, which is the glass temperature of THF (Figure 1). While decreasing the temperature from 300 K down to 170 K, we were able to observe three distinct temperature ranges (see Table 2 for an overview of all relevant temperatures and shifts).

Table 2. Overview of the Corresponding Concrete Values of the Discussed Three Temperature Ranges for Three Samples with Low Polydispersity

polymer	range 1 Abs (Pl) (K)	range 2 (K)	range 3 (K)
P3HT-19	300–270 (280)	265–250	250–170
P3HT-11	300–260 (270)	250–230	230–170
P3HT-5	300–230 (250)	220–200	200–170

At 300 K, the absorption spectra are broad and structureless. When cooling from 300 K to the onset of the phase transition (temperature range 1), the maxima of the spectra feature a red shift by 35–50 meV, accompanied by an increase in intensity of about 10%.

When further decreasing the temperature and entering the temperature range 2, a vibrational resolved absorption spectrum appears with a S_1-S_0 0–0 feature (A_1) at 2.0 eV and a

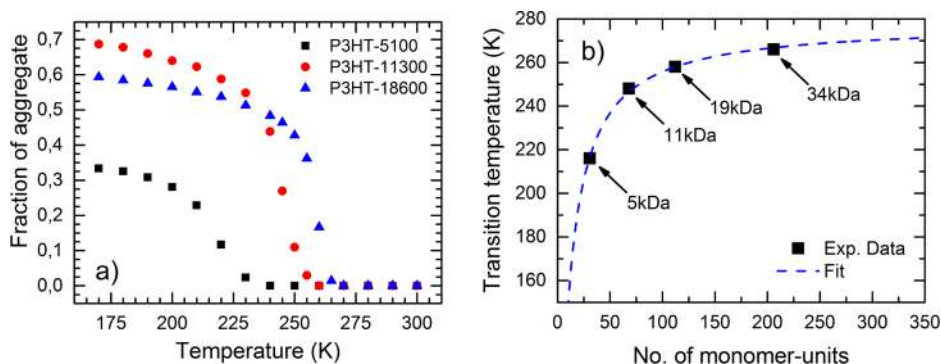


Figure 2. (a) Fraction of aggregates in the solution as a function of temperature for the three different P3HTs. (b) The dependence between the critical transition temperature and molecular weight and a fit using eq 2.

vibrational satellite at 2.2 eV (A_2 feature). At the same time, absorption from the high energy region (above 2.5 eV) is decreasing and an isosbestic point at about 2.5 eV is observed. These main spectral changes take place within a small temperature range of approximately 20–30 K. Upon subsequent cooling, the A_1 -Peak shifts toward lower energies and becomes more intense.

At 300 K, all the fluorescence spectra are more structured compared to the corresponding absorption spectra with a main emission peak at approximately 2.16 eV and a second peak at about 1.99 eV. Within temperature range 1, i.e., between 300 K and the onset of the phase transition, the emission of the samples shifts to lower energies and the overall intensity increases. This is in analogy to absorption spectra. Within temperature range 2, a distinct loss of intensity and simultaneously change in the ratio between the peaks at 2.15 and 2.0 eV can be observed. This effect is more pronounced for P3HT-19 and P3HT-11. At temperatures below the phase transition (temperature range 3), a structured low energy emission spectra can be observed. For both P3HT-19 and P3HT-11 emission from the former pronounced peak at 2.15 eV vanishes. Instead a low energy peak at 1.9 eV appears at 240 K that shifts to 1.8 eV at 170 K. This is complementary to the behavior of the low energy peak observed in corresponding absorption spectra. In contrast to P3HT-19 and P3HT-11 within this temperature range, the emission spectrum of P3HT-5 is more intense and basically retains its original structure except for additional spectral broadening.

In general, the broad absorption and corresponding emission spectra observed within the first temperature range (e.g., at 300 K) can be associated with P3HT chains in the coiled state,^{13,14} while the red-shifted, well-structured absorption and emission spectra observed with the temperature below the phase transition (e.g., at 170 K) are assigned to weakly interacting H-type aggregates in which the chains are more planar and more extended.^{15–18} Therefore, we interpret the data shown in Figure 1 as the signature of a temperature-induced stepwise phase transition from coiled phase toward aggregated P3HT. The observed initial red shift within the first temperature range is associated with an increase in conjugation length of the coiled phase,¹⁹ and a concomitant increase in oscillator strength of the polymer chains.²⁰ This is the signature of an initial planarization process of the coiled chains within the first temperature range. The existence of an isosbestic point at 2.5 eV in the absorption spectra within the second temperature regime indicates that P3HT chains are gradually transformed from coiled to an aggregated state.²¹ Within the temperature range 3 the

aggregate absorption spectra bear out a further redshift. This can be a signature of an increase in conjugation length due to an improved planarization of the aggregates or to spectral diffusion due to energy transfer within aggregates. The strong decrease in overall intensity compared to emission from coiled phase demonstrates that in the aggregated phase the chains form H-aggregates.⁸

In order to further investigate the temperature-dependent conformational behavior of P3HT in solution, the measured absorption spectra were deconvoluted into the spectra of the aggregated and coiled polymer chains, following the approach of Scharich et al.²² Here the absorption spectrum of pure coiled phase was scaled to the high energy shoulder of the respective spectra and subtracted acquiring the fraction of pure aggregate absorption. Taking into account the difference of oscillator strength between coiled and aggregated polymer chains as described in the Supporting Information, the fraction of aggregates f_{aggr} in solution was obtained as a function of temperature for all three samples (Figure 2a). Here we can see that aggregation starts at lower temperatures for lower molecular weights (P3HT-19 at 265 K, P3HT-11 at 255 K, and P3HT-5 at 230 K). Below these temperatures, all samples show a steep increase in aggregate fraction within a temperature range of about 20–30 K. After that, the fraction of aggregate saturates for these three samples toward the lowest measured temperature. At 170 K, the maximum fraction of aggregates reached is 60% for P3HT-19, 70% for P3HT-11, and 32% for P3HT-5. These values (especially for P3HT-19 and P3HT-11) are consistent with typical values found in the literature,^{8,22,23} indicating that the maximum fraction of aggregate is independent of the way the samples are prepared.

The experiments demonstrate that molecular weight of the polymers used has a significant influence on which temperature the transition takes place. We infer the critical temperature from the inflection point in the fraction of aggregate as a function of temperature:

$$\left. \frac{\partial^2 f_{\text{aggr}}}{\partial T^2} \right|_{T_c} = 0 \quad (1)$$

Figure 2b shows that the obtained critical temperatures T_c increase as a function of the number of monomer units for four polymers.

Based upon mean field theory, Sanchez showed that an infinite chain undergoes a second-order phase transition from a swollen coil to a collapsed globule upon cooling below a critical

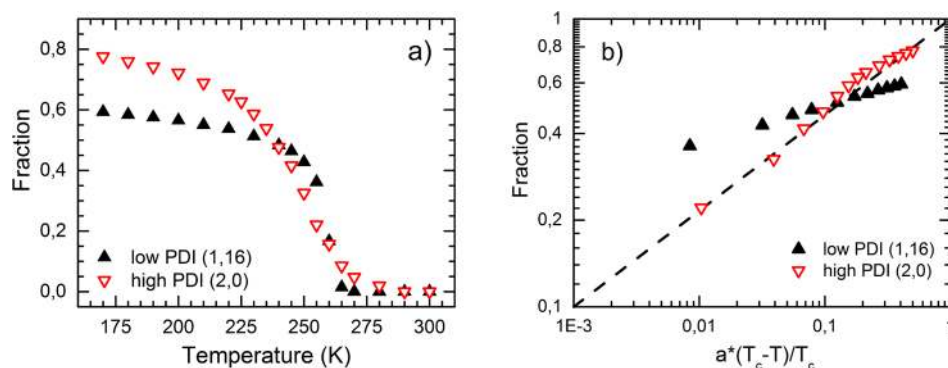


Figure 3. Comparison between the fraction of aggregates of P3HT-19 with low PDI and P3HT-COM with high PDI, (a) as a function of temperature, and (b) as a function of the reduced temperature $a((T_c - T)/T_c)$ plotted double logarithmically. Here, the dashed line indicates the expected course for a second order phase transition.

(transition) temperature T_c .²⁴ In finite systems, this transition becomes pseudo-second order and depends on the chain stiffness. The theory predicts that the critical temperature scales with the number of repeat units N of the chains as

$$\frac{\theta - T_c}{T_c} = \frac{\varphi}{\sqrt{N}} \quad (2)$$

where φ is a constant that depends on the chain stiffness and the so-called theta temperature θ is the critical temperature of an infinite chain. Figure 2b shows that eq 2 provides an excellent fit for T_c as a function of the monomer units and thus the molecular weight of the polymer chains, with fitting parameters $\varphi = 8.7 \pm 0.3$ and $\theta = (278 \pm 1)$ K.

Experiments on samples with similar molecular weight yet different polydispersity (P3HT-COM) shed further light on the nature of this transition. Figure 3a reveals clear differences regarding the temperature dependence of the fraction of aggregates. On one hand, the maximum fraction of aggregate at around 77% for P3HT-COM at a temperature of 170 K is approximately 20% higher compared to the corresponding value for P3HT-19. Furthermore, the shape of the transition seems to be more undefined and more continuous for the P3HT-COM sample compared to the samples with low polydispersity. By contrast, the critical temperatures T_c for the samples with low and high polydispersity are nearly identical, indicating that in this case polydispersity plays no role. If a coil-globule transition in an infinite chain was a second-order transition, it should be described by

$$f_{\text{aggr}}(T) \sim \left(\frac{T_c - T}{T_c} \right)^a, \quad a = 0.33 \quad (3)$$

where f_{aggr} is the fraction of the ordered chains.³ In order to identify the order of the transition, we plotted f_{aggr} versus the reduced temperature $(T_c - T)/T_c$ on a double logarithmic scale (Figure 3b). The dashed line indicates a slope of 0.33, representing a second-order phase transition. The good quality of the fit for the data of P3HT-COM (PDI = 2.0) is, indeed, reminiscent as a second order phase transition. However, for the sample P3HT-19 with low polydispersity, a clear deviation from the second-order course (dashed line in Figure 3b) is obvious. Therefore, we conclude that polydispersity determines the temperature-dependent shape and any assignment to a second order phase transition is accidental. As the transition temperature depends on molecular weight, obviously a broad distribution of chain lengths for high PDI samples smears out

the shape of the transition. Considering the steep transition for the low PDI sample, we conclude that in the limit of a well-defined chain length the transition is of first order. This is in accordance with the work of Cone et al. on the formation of the β -phase in poly(9,9'-dioctylfluorene) (PFO).⁵

Figure 4 shows that in P3HT-19, there is a hysteresis regarding the fraction of aggregates observed upon sample

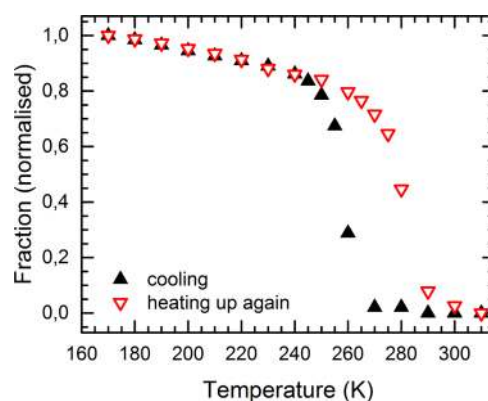


Figure 4. Normalized intensity of the A₁-Peak gathered from absorption spectra while going through a cooling/heating cycle. Waiting time to ensure thermal stability within the solution was set to 45 min between every temperature.

cooling and heating. In order to assess a possible influence of waiting time between two consecutive 10 K temperature jumps, the waiting time was increased up to 90 min. Here we found that the waiting time has virtually no effect on the hysteresis (see SI). This suggests that the hysteresis is linked to an enhanced thermal stability of planarized structures. It was suggested this may be due to side chain ordering occurring after aggregation of the main chains²⁵ which could lead to different polymorphs.²⁶ However, we cannot rule out the possibility that the formation or dissolution of the aggregates during stepwise sample cooling or heating is kinetically hindered which is often the case in first order transitions. Experiments with different heating/cooling rates would be required to tell this possibility.

In summary, we show that the aggregation of P3HT in solution by lowering temperature can be described as a phase transition from coiled phase toward aggregated P3HT. The process is a sequence of swelling of the coiled phase, formation of aggregates, and further planarization of the aggregate. This is consistent with recent simulation of the initial crystallization

process of P3HT in solution.²⁵ The authors conclude that this nucleation process is the sequence of three steps, i.e., ring orientation, elongation of the main chain and, finally ordering the side chains. The bathochromic shift of the unstructured absorption spectrum of P3HT above T_c is likely to be a signature of the first step. We find that the subsequent elongation of the chains and their concomitant collapse to ordered aggregates appears as a thermodynamic first order process.

Our results are corroborated by Monte Carlo simulations by Kolinski and co-workers, who contrast the nature of the coil-globule transition for flexible and for stiffer polymers.²⁷ They find that, whereas flexible chains collapse to an essentially Gaussian, tight random coil, finite length polymers that have a considerable degree of stiffness collapse into an ordered state such as a rod-like bundle. Kolinski et al. compare this collapse to the denatured-to-native transition in globular proteins. The simulations predict that upon lowering the temperature, the dimensions of the stiffer chains first increase until the chain suddenly undergoes a pseudo-first-order phase transition to an ordered dense state. Kolinski and co-workers attribute the initial increase in chain dimension to the dominance of freezing out rotational degrees of freedom over attractive interactions. They suggest this prepares the chain just above the transition in conformation composed of stiff sections connected by “flexible” linkages, which thus primes the polymer to collapse into an ordered structure.

The dependence between molecular weight of the used polymer and the critical temperature of the transition can be rationalized in terms of the theory of Sanchez. In samples with higher polydispersity, realized in commercial samples, there is a superposition of different transition temperatures of chains of different lengths. This obscures the first-order character of the transition. The hysteresis regarding the fraction of ordered chains upon undergoing cooling/heating cycles is tentatively attributed to side chain ordering.

■ ASSOCIATED CONTENT

● Supporting Information

Determination of oscillator strength in the aggregate, impact of waiting time on the hysteresis of the fraction of aggregates. This material is available free of charge via the Internet at <http://pubs.acs.org>.

■ AUTHOR INFORMATION

Corresponding Author

*E-Mail: anna.koehler@uni-bayreuth.de.

Notes

The authors declare no competing financial interest.

■ ACKNOWLEDGMENTS

We acknowledge financial support by the Bavarian State Ministry of Science, Research, and the Arts through the Collaborative Research Network ‘Solar Technologies go Hybrid’ and by the German Science Foundation DFG through the doctoral training center GRK1640. We thank Günter Reiter from Albert-Ludwigs-Universität Freiburg for helpful discussion.

■ REFERENCES

(1) Rughooputh, S. D. D. V.; Bloor, D.; Phillips, D.; Jankowiak, R.; Schütz, L.; Bäessler, H. Fluorescence Studies of Polydiacetylenes in 2-

Methyltetrahydrofuran Vitreous Glasses at Low Temperatures. *Chem. Phys.* **1988**, *125*, 355–373.

(2) Chance, R. R.; Patel, G. N.; Witt, J. D. Thermal Effects on the Optical Properties of Single Crystals and Solution-Cast Films of Urethane Substituted Polydiacetylenes. *J. Chem. Phys.* **1979**, *71*, 206–211.

(3) Köhler, A.; Hoffmann, S. T.; Bäessler, H. An Order-Disorder Transition in the Conjugated Polymer MEH-PPV. *J. Am. Chem. Soc.* **2012**, *134*, 11594–11601.

(4) Pichler, K.; Halliday, D. A.; Bradley, D. D. C.; Burn, P. L.; Friend, R. H.; Holmes, A. B. Optical Spectroscopy of Highly Ordered Poly(*p*-phenylene vinylene). *J. Phys.: Condens. Matter* **1993**, *5*, 7155.

(5) Cone, C. W.; Cheng, R. R.; Makarov, D. E.; Vanden Bout, D. A. Molecular Weight Effect on the Formation of Beta Phase Poly(9,9'-dioctylfluorene) in Dilute Solutions. *J. Phys. Chem. B* **2011**, *115*, 12380–12385.

(6) Ferreira, B.; da Silva, P. F.; Seixas de Melo, J. S.; Pina, J.; Macanita, A. Excited-State Dynamics and Self-Organization of Poly(3-hexylthiophene) (P3HT) in Solution and Thin Films. *J. Phys. Chem. B* **2012**, *116*, 2347–2355.

(7) Berson, S.; De Bettignies, R.; Bailly, S.; Guillerez, S. Poly(3-Hexylthiophene) Fibers for Photovoltaic Applications. *Adv. Funct. Mater.* **2007**, *17*, 1377–1384.

(8) Clark, J.; Chang, J.-F.; Spano, F. C.; Friend, R. H.; Silva, C. Determining Exciton Bandwidth and Film Microstructure in Polythiophene Films Using Linear Absorption Spectroscopy. *Appl. Phys. Lett.* **2009**, *94*, 163306.

(9) Duong, D. T.; Ho, V.; Shang, Z.; Mollinger, S.; Mannsfeld, S. C. B.; Dacuña, J.; Toney, M. F.; Segalman, R.; Salleo, A. Mechanism of Crystallization and Implications for Charge Transport in Poly(3-ethylhexylthiophene) Thin Films. *Adv. Funct. Mater.* **2014**, n/a–n/a.

(10) Khan, A. L. T.; Sreearunothai, P.; Herz, L. M.; Banach, M. J.; Köhler, A. Morphology-Dependent Energy Transfer within Polyfluorene Thin Films. *Phys. Rev. B* **2004**, *69*, 085201.

(11) Lohwasser, R. H.; Thelakkat, M. Toward Perfect Control of End Groups and Polydispersity in Poly(3-hexylthiophene) via Catalytic Transfer Polymerization. *Macromolecules* **2011**, *44*, 3388–3397.

(12) Singh, C. R.; Gupta, G.; Lohwasser, R.; Engmann, S.; Balko, J.; Thelakkat, M.; Thurn-Albrecht, T.; Hoppe, H. Correlation of Charge Transport with Structural Order in Highly Ordered Melt-Crystallized Poly(3-hexylthiophene) Thin Films. *J. Polym. Sci., Part B: Polym. Phys.* **2013**, *51*, 943–951.

(13) Hotta, S.; Rughooputh, S. D. D. V.; Heeger, A. J.; Wudl, F. Spectroscopic Studies of Soluble Poly(3-alkylthienylenes). *Macromolecules* **1987**, *20*, 212–215.

(14) Brown, P. J.; Thomas, D. S.; Köhler, A.; Wilson, J. S.; Kim, J.-S.; Ramsdale, C. M.; Sirringhaus, H.; Friend, R. H. Effect of Interchain Interactions on the Absorption and Emission of Poly(3-hexylthiophene). *Phys. Rev. B* **2003**, *67*, 064203.

(15) Clark, J.; Silva, C.; Friend, R. H.; Spano, F. C. Role of Intermolecular Coupling in the Photophysics of Disordered Organic Semiconductors: Aggregate Emission in Regioregular Polythiophene. *Phys. Rev. Lett.* **2007**, *98*, 206406.

(16) Park, Y. D.; Lee, H. S.; Choi, Y. J.; Kwak, D.; Cho, J. H.; Lee, S.; Cho, K. Solubility-Induced Ordered Polythiophene Precursors for High-Performance Organic Thin-Film Transistors. *Adv. Funct. Mater.* **2009**, *19*, 1200–1206.

(17) Oh, J. Y.; Lee, T. I.; Myoung, J.-M.; Jeong, U.; Baik, H. K. Coating on a Cold Substrate Largely Enhances Power Conversion Efficiency of the Bulk Heterojunction Solar Cell. *Macromol. Rapid Commun.* **2011**, *32*, 1066–1071.

(18) Spano, F. C. Absorption in Regio-Regular Poly(3-hexyl)-Thiophene Thin Films: Fermi Resonances, Interband Coupling and Disorder. *Chem. Phys.* **2006**, *325*, 22–35.

(19) Hoffmann, S. T.; Bäessler, H.; Köhler, A. What Determines Inhomogeneous Broadening of Electronic Transitions in Conjugated Polymers? *J. Phys. Chem. B* **2010**, *114*, 17037–17048.

(20) Valeur, B. Absorption of UV–Visible Light. In *Molecular Fluorescence*; Wiley-VCH Verlag GmbH: Weinheim, Germany, 2001; pp 20–33.

(21) Cohen, M. D.; Fischer, E. 588. Isosbestic Points. *J. Chem. Soc. (Resumed)* **1962**, 3044.

(22) Scharsich, C.; Lohwasser, R. H.; Sommer, M.; Asawapirom, U.; Scherf, U.; Thelakkat, M.; Neher, D.; Köhler, A. Control of Aggregate Formation in Poly(3-hexylthiophene) by Solvent, Molecular Weight, and Synthetic Method. *J. Polym. Sci., Part B: Polym. Phys.* **2012**, *50*, 442–453.

(23) Nagarjuna, G.; Baghgar, M.; Labastide, J. A.; Algaier, D. D.; Barnes, M. D.; Venkataraman, D. Tuning Aggregation of Poly(3-hexylthiophene) within Nanoparticles. *ACS Nano* **2012**, *6*, 10750–10758.

(24) Sanchez, I. C. Phase Transition Behavior of the Isolated Polymer Chain. *Macromolecules* **1979**, *12*, 980–988.

(25) Takizawa, Y.; Shimomura, T.; Miura, T. Simulation Study of the Initial Crystallization Processes of Poly(3-hexylthiophene) in Solution: Ordering Dynamics of Main Chains and Side Chains. *J. Phys. Chem. B* **2013**, *117*, 6282–6289.

(26) Koch, F. P. V.; Heeney, M.; Smith, P. Thermal and Structural Characteristics of Oligo(3-hexylthiophene)s (3HT)_n, n = 4–36. *J. Am. Chem. Soc.* **2013**, *135*, 13699–13709.

(27) Kolinski, A.; Skolnick, J.; Yaris, R. The Collapse Transition of Semiflexible Polymers. A Monte Carlo Simulation of a Model System. *J. Chem. Phys.* **1986**, *85*, 3585–3597.